Evaluation of an Electroless Nickel Interlayer On the Fatigue & Corrosion Strength Of Chromium-plated AISI 4340 Steel

M.P. Nascimento, H.J.C. Voorwald, R.C. Souza & W.L. Pigatin

Despite the fact that chromium electrodeposition results in protection against wear and corrosion, combined with chemical resistance and good lubricity, the reduction in fatigue strength of base metal and environmental requirements causes one to search for possible alternatives. To improve the fatigue and corrosion resistance of AISI 4340 steel, an experimental study has been made for an intermediate electroless nickel layer deposited on base metal. The objective of this study was to analyze the effect of nickel underplate on the fatigue and corrosion strength of hard-chromium-plated AISI 4340 steel. Deposition of the conventional wear-resistant hard chromium plating leads to a decrease in mechanical properties of the base metal, especially the fatigue strength. Rotating bending fatigue tests results indicate better performance for conventional hard chromium plating. Good corrosion resistance in salt fog exposure was obtained for the accelerated hard chromium plating. Experimental data showed higher fatigue and corrosion resistance for samples prepared with accelerated hard chromium plate over electroless nickel plate, when compared with samples without electroless nickel underplate.

Although problems concerning chromium plating have resulted in searches to identify economically viable hard chromium alternatives, chromium plating is a well-established and high-quality electrodeposited coating used to guarantee high levels of hardness, resistance to wear and corrosion, and low coefficient of friction in several applications.[1-4]

The excellent corrosion and wear resistances offered by hard chromium plating are related to the passive film of Cr_2O_3. The passivated film on chromium plating can result in a barrier to hydrogen diffusion, preventing hydrogen embrittlement.[5] The tensile stresses in electroplated chromium coatings resulting from the deposition process are relieved by local microcracking during electroplating.

It was observed that the residual stresses are in some way affected by the substrate, but only at the interface. They decrease with the depth of the coating and increase again at the coating/substrate interface.[6] Microcracks, which form during electrodeposition when the tensile stress exceeds the cohesive strength of the chromium, are responsible for the stress relief in the deposit.[7]

Experimental results from bending fatigue tests on samples with different coatings and coating conditions indicate that the fatigue strength after cycling is dependent on the fracture behavior of the substrates and on the hardness and residual stresses at the substrate surface.

Deterioration of the fatigue strength was observed for chromium plating.[8] Compressive residual stresses that are obtained by surface plastic deformation are responsible for the increase in fatigue strength in shot-peened mechanical components.[9] Compressive residual stresses induced by machining processes also result in improvement in the fatigue resistance of AISI 4340 steel.[10] Increase in the fatigue crack propagation resistance in AISI 4340 steel with electron beam surface hardening was associated with residual stress distribution and microstructural characteristics.[11]

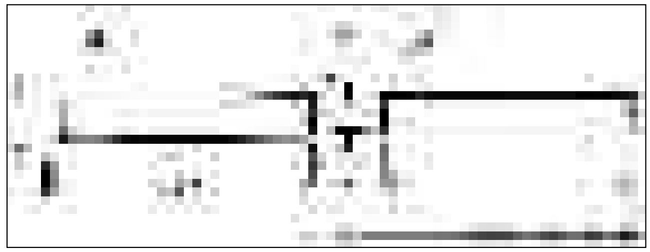

Fig. 1—Rotating bending fatigue testing specimens.

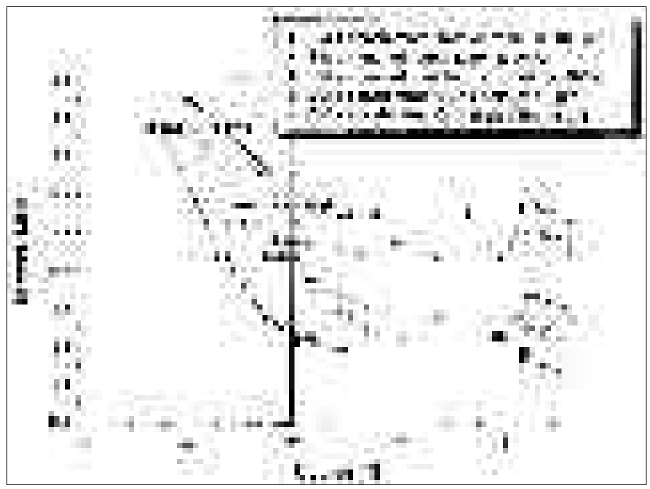

Fig. 2—S-N curves for rotating bending fatigue tests.

An experimental program conducted with samples of an AISI 1045 plain carbon steel, uncoated and coated with electroless nickel deposits containing approximately 10-percent phosphorus and about 20 µm thickness, indicated an increase in the fatigue strength of the substrate in the stress range of 221 to 331 MPa in the presence of an aqueous solution of three percent NaCl.[12]

The influence of the electroless Ni-P deposit thicknesses ranging between 7 and 37 µm is to reduce the fatigue strength of the coated substrate associated, probably, with the development of tensile residual stresses during the growth of the deposits.[13] As a consequence of the observations concerning chromium plating, recent advances in high-velocity oxygen fuel (HVOF) technology offer a safer and cleaner alternative, with better corrosion resistance. In the case of fatigue and friction tests, the results were acceptable, indicating interesting perspectives in the use of tungsten carbide coating to replace chromium plating.[1] Experimental results indicate that the application of plasma-sprayed Ni-based composite WC coatings, increases the abrasive wear resistance in comparison with the traditional materials.[14]

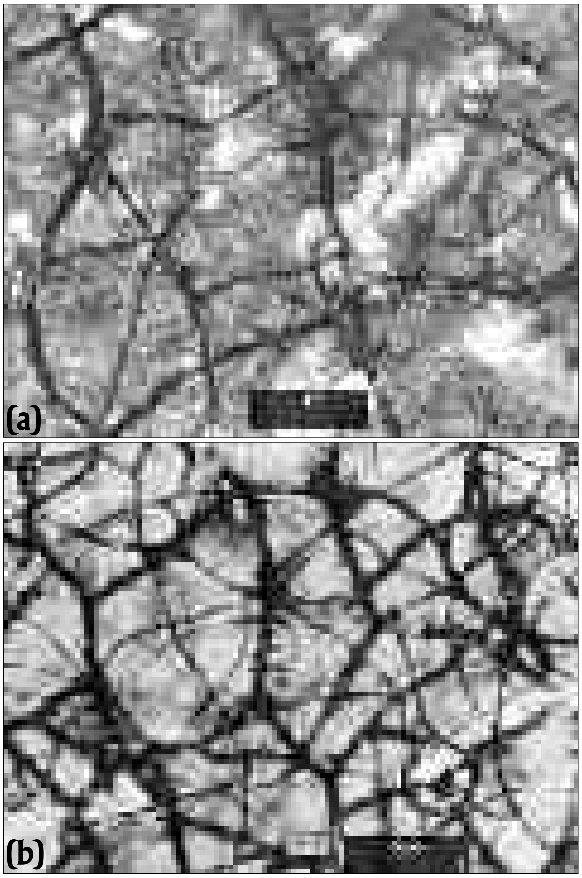

Fig. 3—Microcrack surface network in conventional (a) and accelerated (b) hard chromium electroplatings. Anodic etching from 15 to 30 A/dm^2 for 30 sec 400X.

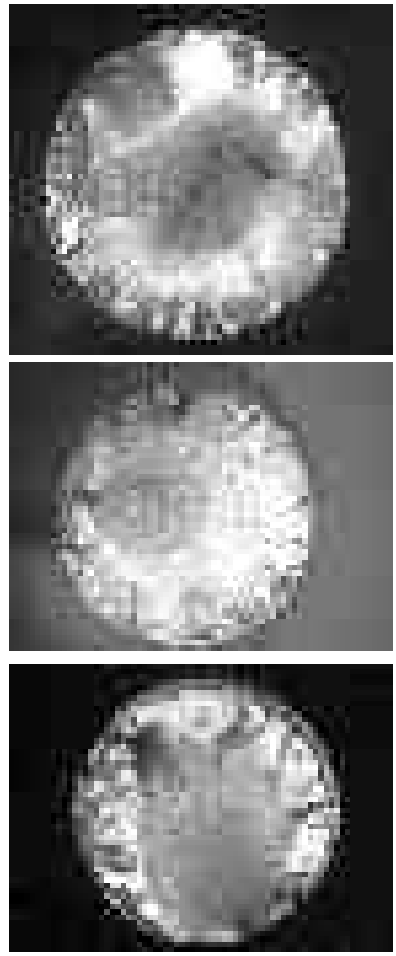

Fig. 4—Fracture surface from bending fatigue specimens electroplated with:

(a) electroless nickel underplate, 13 µm thick, and accelerated hard chromium electroplated, 10 µm thick;

(b) accelerated hard chromium, 100 µm thick, and

(c) electroless nickel underplate, 15 µm thick, and accelerated hard chromium electroplated, 145 µm thick and tested at 78 percent σ_e (871 MPa).

Protection against corrosion is an important parameter in the aerospace industry. Experimental tests conducted to determine corrosion resistance according to ASTM B117 on steel panels indicate better protection for tin-zinc electroplated coatings than for other coatings.[15] A reduction in the fatigue strength by 39 percent was observed as a result of electroless Ni-P alloy plating on quenched and tempered 30 CrMoA steel. The fatigue strength was increased by 30 percent for the shot-peened specimens compared with direct plating. The interface between the coating and the substrate is an important region, considering fatigue crack nucleation.[16]

The objective of this study was to compare the fatigue strength, abrasive wear and corrosion resistance of AISI 4340 steel coated with conventional and accelerated electroplated chromium. The effect of nickel underplate on the fatigue and corrosion strength of AISI 4340 steel with accelerated hard chromium plate was also investigated. S-N curves were obtained in rotation bending, for the base metal, with both conventional chromium plating conditions and accelerated chromium plating with an electroless nickel-plated layer deposited on the base metal.

Experimental Procedure

AISI 4340 steel is widely used in the aircraft industry for fabrication of critical components, where strength and toughness are fundamental design requirements. Chemical analysis of the material used in this research indicates accordance with specifications.

The fatigue experimental program was performed on rotating bending fatigue test specimens machined from hot-rolled, quenched and tempered bars, according to Fig. 1. The specimens were polished in the reduced section with 600-grit papers, inspected dimensionally and by magnetic particle inspection. Fatigue tests specimens were quenched from 815 to 845ºC in oil (20ºC) and tempered in the range of 520 ±5 ºC for two hours.

Mechanical properties of the material after the heat treatment were: hardness of 39 HRC; yield tensile strength of 1118 MPa and ultimate tensile strength of 1210 MPa. After final preparation, samples were subjected to a stress-relieve heat treatment at 190ºC for 4 hours to reduce residual stresses induced by machining. Average superficial roughness in the reduced section of the samples was R_a ~ 2.75 µm, with standard deviation of 0.89 µm.

Rotating bending fatigue tests were conducted using a sinusoidal load at 50 Hz and load ratio R = -1, at room temperature, considering as fatigue strength the specimen's complete fracture or 10^7 load cycles.

Five groups of fatigue specimens were prepared to obtain S-N curves for rotating bending fatigue tests:

1. Smooth samples of base metal.
2. Samples of base metal with conventional hard chromium electroplating, 160 µm thick.
3. Samples of base metal with accelerated hard chromium electroplating, 100 µm thick.
4. Samples of base metal with intermediate electroless nickel plating layer, 13 µm thick and electroplated with accelerated hard chromium, 10 µm thick.
5. Samples of base metal with intermediate electroless nickel plating layer, 15 µm thick, and electroplated with accelerated hard chromium, 145 µm thick.

Table 1
Number of Cycles to Failure

Stress (Mpa)	Base Metal Cycles	10 µm Cr/13 µm Ni Cycles	% BM	145 µm Cr/15 µm Ni Cycles	% BM	Conventional Cr Cycles	% BM	Accelerated Cr Cycles	% BM
850	22000	28000	127	13000	59	9500	43	6000	27
750	60000	50000	83	23000	38	18000	36	9000	18
650	299000	90000	30	43000	14	36500	12	14200	5

Salt Spray Test

The performance of the coatings was evaluated with respect to chemical corrosion resistance in specific environments. The test panels were prepared from normalized AISI 4130 steel 254 mm in length, 76 mm width and 1 mm thickness, under the following conditions:

- Accelerated hard chromium electroplating: 16, 36 and 49 µm thick
- Conventional hard chromium electroplating: 16, 36 and 49 µm thick
- Accelerated hard chromium electroplating, 50 µm thick and with electroless nickel plating underlayer 10, 20 and 30 µm thick, respectively.

Samples for chemical corrosion resistance tests were prepared and exposed to a five-percent salt spray test according to ASTM B117. The specimens were supported at 20 degrees from the vertical. The results of the corrosion resistance testing were analyzed by image analysis software.

Abrasive Wear Test

For abrasive wear tests, samples were prepared from normalized AISI 4130 steel, 4 mm in thickness and 100 mm square, according to FED-STD-141, then electroplated with accelerated and conventional hard chromium, 100 µm thick. The tests were conducted in a Taber Abrader, at room temperature, using 1 kg load and a CS-17 abrading wheel. The results were analyzed by wear index (mg/1,000 cycles) and total wear (mg/10,000 cycles) data.

Hard Chromium Electroplating

Conventional hard chromium electroplating was carried out from a chromic acid solution with 250 g/L of CrO_3 and 2.5 g/L of H_2SO_4, at 50 to 55ºC, with a current density from 31 to 46 A/dm^2, and a deposition rate of 25 µm/hr. A bath with a single catalyst based on sulfate was used.

Accelerated hard chromium electroplating was carried out from a chromic acid solution with 250 g/L of CrO_3 and 2.7 g/L of H_2SO_4, at 55 to 60ºC, with a current density of 55 to 65 A/dm^2, and a deposition rate of 80 µm/hr. A bath with double catalyst (one sulfate and the other without fluoride) was used.

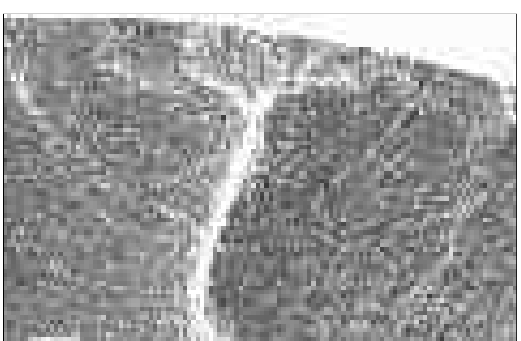

Fig. 5–Fracture surface from a bending fatigue specimen electroplated with accelerated hard chromium, 100 µm thick and fatigue tested at 29 percent σ_{ys}.

After deposition, the samples were subjected to a hydrogen embrittlement relief treatment at 190ºC for 8 hr. The average surface roughness of the hard chromium electroplating was R_a ~ 3.13 µm in the reduced section and standard deviation of 0.79 µm, in the as-plated condition.

For the microcrack determination in both hard chromium electrodeposits, samples were prepared from normalized AISI 4340 steel (R_a ~ 0.2 µm), 1 mm thickness, 25 mm width and length, and with accelerated and conventional hard chromium electroplating, both with 100 µm thickness, which resulted in a surface roughness R_a ~ 0.74 µm for the former and R_a ~ 1.6 µm for the latter, in the as-plated condition. The surface microcracks were enhanced through anodic etching for 30 sec with a current density of 25 A/dm^2 in the same chromium bath and later analyzed using an optical microscope.

All surface roughness data measured in this research was obtained using a cut-off of 0.8 mm. The analysis of fracture surfaces was carried out on rotating bending fatigue specimens by scanning electron microscopy. The metallographic analysis was carried out by optical microscopy.

Electroless nickel deposition was performed in a commercial solution resulting in a coating with high phosphorus content (10 to 12 %P). Preceding this superficial treatment, samples were vapor- and alkaline-degreased and deoxidized in hydrochloric acid solution. After electrodeposition, samples were heat treated at 190ºC for 8 hr to avoid hydrogen embrittlement.

Based on light optical and scanning electronic microscopy of the coating morphology, microcracks formed in hard chromium plating and fatigue cracks were observed.

Results & Discussion

Fatigue Test

The S-N curves for the rotating bending fatigue tests for the base metal and plated specimens are shown in Fig. 2. Figure 2 and Table 1 show that the effect of the coating in the rotating bending fatigue tests is to decrease the fatigue strength of AISI 4340 steel. For high stress levels, the influence is not as significant as at low stress levels.

Experimental data indicate that: (1) accelerated hard chromium plating (100 µm) resulted in the lowest number of cycles to failure from all conditions studied; (2) the negative effect on fatigue behavior increased with coating thickness (10 to 145 µm); and (3) better performance with an intermediate electroless nickel layer on chromium plated samples.

Table 2 shows the fatigue strength for all the coating conditions studied at 10^4, 10^5 and 10^7 cycles, in which the influence of coatings on the low-cycle fatigue, high-cycle fatigue and fatigue limit, is clearly represented. The tensile stresses in electroplated chromium coatings resulting from the deposition process and relieved by local microcracking during electroplating, and crack propagation from coatings to the substrate, indicating strong adhesion, are factors

Table 2
Fatigue Strength at 10^4, 10^5 & 10^7 Cycles

Conditions	Fatigue Strength (Mpa) 10^4	10^5	10^7
Base Metal	950 (85% σ_{ys})	700 (63% σ_{ys})	615 (55% σ_{ys})
Accel. Cr (10 µm) Ni (13 µm)	>1000 (127% σ_{ys})	640 (57% σ_{ys})	522 (47% σ_{ys})
Accel. Cr (145 µm) Ni (15 µm)	900 (80% σ_{ys})	525 (47% σ_{ys})	366 (33% σ_{ys})
Conv. Cr (160 µm)	840 (75% σ_{ys})	500 (45% σ_{ys})	321 (29% σ_{ys})
Accel. Cr (100 µm)	730 (65% σ_{ys})	340 (30% σ_{ys})	280 (25% σ_{ys})

Table 3
Through Thickness Vickers Microhardness with 1 N Load

Coatings	Microhardness – VHN_{1N} Surface	Core	Interf. from Coating	Interf. from Base Metal
Accel. Cr (100 µm)	864	920	913	396
Conv. Cr (160 µm)	897	906	912	376
Accel. Cr (145 µm)/ Ni (15 µm)	847	870	920 Ni = 452	427

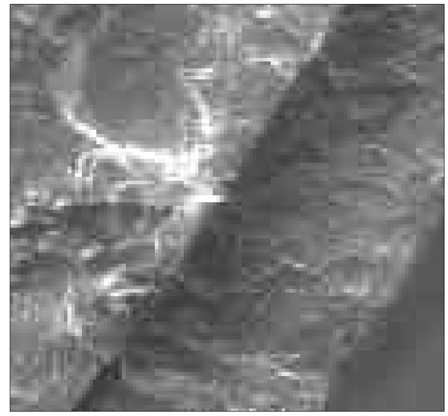

Fig. 6—Fracture surface from a bending fatigue specimen electroplated with accelerated hard chromium, 100 µm thick and fatigue tested at 78 percent σ_{ys}.

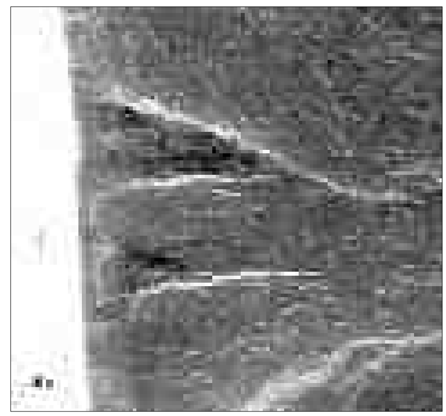

Fig. 7—Fracture surfaces of samples with electroless nickel underplate, 13 µm thick, and accelerated hard chromium, electroplated 10 µm thick and fatigue tested at 55 percent σ_{ys}.

responsible for the decrease in fatigue strength, when compared with base metal.

Considering both hard-chromium-electroplated rotating bending fatigue results, the negative influence of coating on the fatigue strength of the steel can be seen. From analysis of these two coatings, it is possible to observe the better performance of the conventional hard chromium plating in relation to the accelerated hard chromium plating, despite the greater thickness of the former. This may be attributed to the lower microcrack density compared to the accelerated hard chromium plating, as shown in Fig. 3.

The microcrack density quantitative analysis indicated median values of 1512 microcracks/cm and a standard deviation of 190.6 microcracks/cm for the accelerated hard chromium plating, and 223 microcracks/cm with a standard deviation of 57.5 microcracks/cm for conventional hard chromium plating. Microcracks form when the high tensile residual internal stresses exceed the cohesive strength of the chromium deposits and affect the fatigue behavior of a plated part.

Thus, microcrack density arises as a relief of the tensile residual internal stress, which increases when the chromium thickness increases. Pina *et al.*[6] show that the microcrack density changes along the thickness, being higher in the core and lower in the surface of the coating and in the substrate/coating interface, as a result of the imbalance between the residual stresses. On the surface of the coating, the microcracks arise in a network format, without preferential direction and characterizing an equi-biaxial residual stress state. With respect to residual stresses, an inverse behavior from that observed for the microcracks occurred.

In general, the higher the microcrack density is, the higher is the tensile residual internal stresses and/or their relief. This means that the accelerated hard chromium plating is responsible for higher tensile residual internal stresses and/or presents the highest crack initiation/propagation front amount. The different microcrack density between both kinds of hard chromium plating produced practically the same effect in low-cycle fatigue, however, because crack growth occurs after a few cycles of fatigue testing.

The fatigue strength for the two conditions studied was reduced because of the high tensile residual internal stresses, microcrack density and high adhesion coating/substrate interface, which allow crack growth from the coating through the interface into the base metal. The results for rotating bending fatigue tests for samples with an intermediate electroless nickel plating layer of 13 and 15 µm thickness and accelerated hard chromium plated with 10 and 145 µm thickness, respectively, indicate higher fatigue strength for the lower chromium thickness. As stated before, the tensile residual stresses in electroplated chromium coatings are related to the thickness, decreasing the fatigue strength of AISI 4340 steel.

Comparison of these results with 100 µm chromium plating indicates that the fatigue strength, after cycling, is dependent on the fracture behavior of the substrates and on the interaction between coatings. The electroless nickel plating underlayer is responsible for the increase in fatigue strength of AISI 4340 steel plated with chromium, as a result of higher toughness and compressive residual stresses. These stresses delayed the crack propagation from the external accelerated hard chromium plating in the direction of the base metal. The residual stresses, present in electroless nickel plating, are related to the phosphorus content, being tensile between four and nine %P and compressive for content lower than 4% P and in the range 10 to 12 %P.[17]

Fatigue crack nucleation and propagation, normally starting at the interface of coating and substrate, are influenced by compressive residual stresses in a positive way.[16] Rotating bending fatigue tests in AISI 1045 steel, nickel coated (10 %P), seven µm thick and post-treated at 200ºC for one hr, resulted in better fatigue behavior when compared with the 17 and 37 µm thicknesses.[13] A better corrosion-fatigue (in 3% NaCl) performance in rotating bending tests was obtained for AISI 1045 steel coated with 20 µm of electroless nickel (10 %P) and post-treated at 200ºC for four hours. In the same study, an increase was also observed in the coated hardness from 637 to 772 HVN after heat treatment to avoid hydrogen embrittlement, indicating possible precipitation of Ni_3P and influence on the residual stresses.

The reduction in the fatigue strength in samples plated with chromium with an electroless nickel plating interlayer, compared with the base metal, may be associated with a reduction in the compressive residual stresses in the electroless nickel layer resulting from the heat treatment. Therefore, they were not able to compensate the tensile residual stresses in the accelerated hard chromium plating. It is possible to observe, in Fig. 2, that in low-cycle fatigue ($N < 10^4$ cycles), a 13-µm-thick electroless nickel plating interlayer increased the fatigue strength, probably as a result of an interaction between the compressive residual stresses in the electroless nickel plating and the tensile residual stresses present in the accelerated hard chromium coating.

Table 4
Salt Spray Test Results After 24, 48 & 72 hr

Coating		Salt Spray Test (Corroded Area, %) Accelerated Hard Chromium			Conventional Hard Chromium		
		16µm	36µm	49µm	16µm	36µm	49µm
Time, hr	24	80%	10%	OK	90%	70%	50%
	48	100%	30%	5%	100%	100%	100%
	72	100%	100%	100%	100%	100%	100%

Table 5
Salt Spray Test Results for Samples With Electroless Nickel Plating Underlayer

Sample Ni, µm	Corroded Area, % 24 hr	48 hr	120 hr	144 hr	168 hr	216 hr	288 hr	312 hr
10	OK	OK	OK	10	30	50	70	80
20	OK	OK	OK	OK	OK	OK	OK	OK
30	OK	OK	OK	OK	OK	OK	OK	OK

Results of the influence of hard chromium multilayer on crack propagation indicate differences in performance compared to hard chromium electroplated with the one thickness only; associated, probably, with the induced residual stresses profile.[18] Figure 4 shows typical fracture surfaces from samples tested in rotating bending, indicating that fatigue crack nucleation started at the free surface. Figures 4a, 4b and 4c are related to samples that were accelerated-hard-chromium-plated 10 µm thick with an electroless nickel underlayer 13 µm thick; accelerated-hard-chromium-plated 100 µm thick and accelerated-hard-chromium-plated 145 µm thick with electroless nickel underlayer 15 µm thick, respectively.

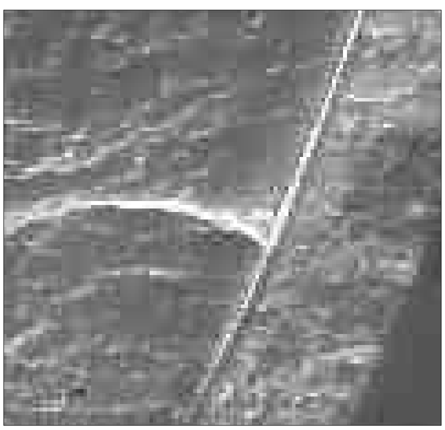

Fig. 8—Fracture surface of rotating bending fatigue samples with electroless nickel underplate, 15 µm thick, and accelerated hard chromium electroplated, 145 µm thick, and tested at 871 MPa.

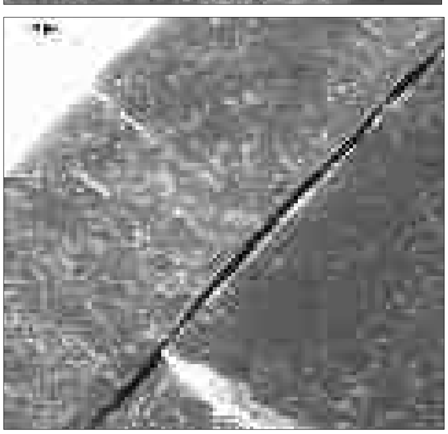

Fig. 9—Fracture surface of rotating bending fatigue samples with electroless nickel underplate, 15 µm thick, and accelerated hard chromium electroplated, 145 µm thick, and tested at 871 MPa.

It is possible to observe, in all cases, the same characteristic of fatigue crack nucleation and propagation all around the specimen, indicating several crack fronts acting during the fatigue tests. This behavior may be associated with the microcrack density in hard-chromium-electroplated specimens. From Fig. 5, which represents a fracture surface from a rotating bending fatigue specimen plated with accelerated hard chromium and tested in high cycle, cracks can be seen starting at the free coating surface, at the middle of chromium plating and at the coating-substrate interface. Fatigue crack coalescence and propagation inside the base metal is also illustrated in Fig. 5.

From Fig. 6, which represents a fracture surface from a rotating bending fatigue specimen electroplated with accelerated hard chromium and tested at 871 MPa, the coating uniform thickness, strong substrate-coating interface and microcracks distributed along thickness in a radial shape can be seen. In the same figure, fatigue crack nucleation at the coating-substrate interface is also represented.

The fracture surface of a sample with electroless nickel underplate 13 µm thick and accelerated-hard-chromium-electroplated 10 µm thick and fatigue-tested at 55 percent σ_{ys}, is indicated in Fig. 7. From this figure, it is possible to observe the electroless nickel layer acting as a barrier to radial linear crack propagation throughout the layer thickness to the base metal. Fatigue cracks starting from the chromium/nickel and nickel/substrate interfaces are also illustrated in Fig. 7.

The fracture surface of rotating bending fatigue samples with electroless nickel underplate 15 µm thick and accelerated-hard-chromium-electroplated 145 µm thick and tested at 871 MPa, are indicated in Figs. 8 and 9. The importance of the electroless nickel underlayer as a barrier to crack propagation is clearly shown in both figures, as well as the strong interface adhesion between the accelerated hard chromium electroplate and the electroless nickel, and the weak interface adhesion between the electroless nickel and the substrate.

In coated specimens, an important characteristic of the rotating bending fatigue tests is that preferential crack growth occurs in the substrate/coating interface, leading to

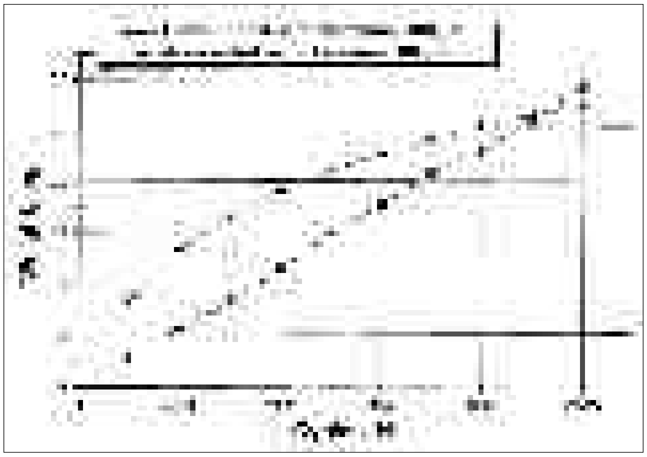

Fig. 10—Abrasive wear weight loss vs. number of cycles.

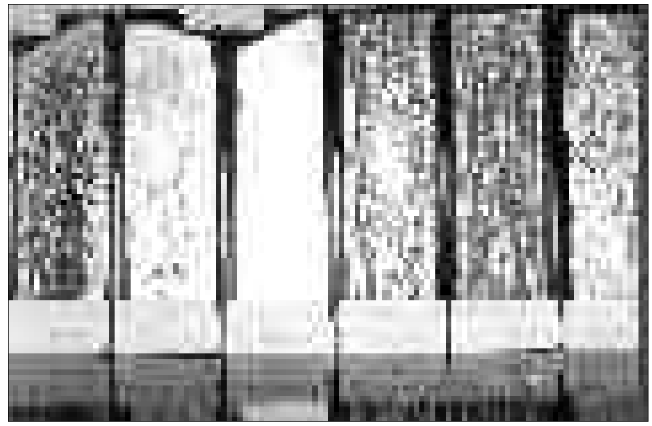

Fig. 11—Salt spray test results for hard chromium electroplated samples after 48 hr.

adherence fracture and possible delamination.[20] The coating delamination at the substrate interface, in different solid materials, may be correlated to the direction in which the crack approaches the interface and the condition of the materials involved, ductile/brittle or vice-versa.[21]

In this study, the experimental results indicate that fatigue cracks in hard chromium electroplating propagate through the substrate/coating interface to the inside of the base metal without interference. Despite the fact that the electroless nickel underlayer acted as a barrier to crack propagation, fatigue cracks from the hard chromium plating propagated through the electroless nickel coating in a radial shape to the substrate, but changed direction at the substrate/coating interface, resulting in delamination. This behavior is associated with the strength of the materials involved (*i.e.*, hard chromium electroplating, electroless nickel and 4340 high strength steel).

Abrasive Wear Tests

The abrasive wear resistance of the accelerated and conventional hard chromium plating was evaluated and the results in terms of wear weight loss are represented in Fig. 10. Comparison of the abrasive wear resistance results shown in Fig. 10 indicate, in the first 1000 cycles, a higher wear weight loss for the accelerated hard chromium electroplating than for the conventional hard chromium electroplating. In the subsequent cycles, however, the wear weight loss of the accelerated hard chromium electroplating decreased with an increase in the number of cycles in a parabolic way, and resulting, after 10,000 cycles, in lower wear weight loss than conventional hard chromium plating. This may be explained by the through-thickness microhardness variation, according to Table 3.

The lower hardness of the accelerated-hard-chromium-plated surface and its increased through-thickness may explain the decrease in the wear weight loss after a number of cycles. For conventional hard chromium plating, the wear weight loss data indicate that no significant variation in the coating microhardness occurred until after 10,000 test cycles. It is likely that the reversal in relation to the conventional hard chromium plating, occurred in hardness change sites. This may also be associated with the higher microcrack density and the higher hardness in the accelerated hard chromium plating, implied by the higher amount of edges, resulting in lower fracture toughness and, consequently, greater brittleness.

In addition, the higher the crack density, the greater the number of previously detached solid particles that are suppressed in the microcracks and that decrease the wear strength. This may have implications for micro-cutting, which is considered to be the predominant wear weight loss mechanism.[14] Hard chromium electroplates with hardness around 750-800 VHN were found to have the best frictional wear resistance, if obtained as deposited or by moderate heat treatment of harder deposits.

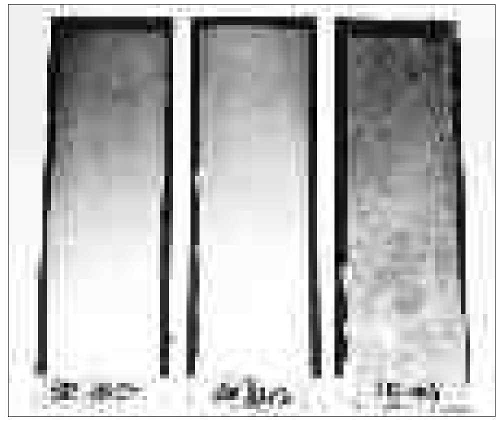

Fig. 12—Salt spray test results for coated samples after 312 hr.

Salt Spray Tests

The results of the corrosion testing, performed in a qualitative way, were obtained by visual inspection of the specimen surface exposed to salt spray. Both hard chromium platings completed the tests with full corrosion. Table 4 and Fig. 11 show the results of the salt spray test for 24, 48 and 72 hr duration. Figure 11 shows clearly the higher salt spray resistance of the accelerated-hard-chromium-plated specimens during all testing.

For the accelerated-hard-chromium-plated specimen 49 µm in thickness and subjected to 48 hours in a salt spray environment, it was observed that its surface showed around five percent corrosion products. Under the same conditions, corrosion of the conventional hard-chromium-plated specimens was complete (*i.e.*, visually 100% corroded). This experimental behavior is associated with the number of microcracks in the deposit in such a way that the greater the number of microcracks, the more discontinuities and, as a result, better protection against corrosion.[7]

Despite the higher microcrack density of the accelerated-hard-chromium-plating, the surface roughness measurements indicate lower values than for the conventional hard-chromium-plating, as mentioned before. In general, the corrosion resistance is associated with the surface roughness of a part (*i.e.*, the greater the surface roughness, the greater the corrosion attack because of greater surface area.[19]

The conventional hard chromium electroplating process therefore yielded lower density and, consequently, more microcracks of greater depth. It is clear that the increased thickness enhanced the hard chromium protection against salt spray corrosion. Here also, however, the substrate was not quite protected against the aggressive action of the salt spray environment. This general corrosion results from the high content of pores and microcracks inherent to the process itself. The pores and microcracks act as canals, leading the corrosive agent to the substrate/coating interface.

The salt spray test results for samples of hard chromium electroplated with an intermediate electroless nickel layer are shown in Table 5 and Fig. 12. Table 6 represents the salt spray test results for samples plated with accelerated hard chromium 50 µm thick and three different electroless nickel plating underlayers 10, 20 and 30 µm thick, respectively. It can be seen that after 144 hours, the sample with an electroless nickel underlayer 10 µm thick showed 10 percent surface corrosion, increasing with testing time.

On the other hand, no visual corrosion was observed on samples with electroless-nickel-plated underlayers of 20 and 30 µm thick after 312 hours of testing. The surface aspect after salt spray testing is shown in Fig. 12. Chitty *et al.*[12] attributed the excellent (10-12 %P) electroless nickel plating behavior in an aggressive environment in the "as-deposited" condition, to its high density, low porosity and amorphous structure. To perform the rotating bending fatigue tests in samples with an intermediate electroless nickel layer and accelerated hard chromium plating, thicknesses of 13 and 15 µm were chosen, based on the salt spray test results.

Findings

- The higher rotating bending fatigue strength of the conventional hard chromium plating compared to the accelerated hard chromium plating, despite the greater thickness of the former, is associated with the lower microcrack density of the conventional hard chromium electroplating.
- The results for rotating bending fatigue tests for samples with an intermediate electroless nickel layers 13 and 15 µm thick, and accelerated hard chromium plating 10 and 145 µm thick, respectively, indicate higher fatigue strength for the lower chromium thickness.
- Experimental results indicate the importance of the electroless nickel underlayer as a barrier to crack propagation
- Abrasive wear test results indicate, in the first 1000 cycles, a higher wear weight loss for the accelerated hard chromium electroplate than for the conventional hard chromium plating. In the subsequent cycles, the wear weight loss of the accelerated hard chromium decreases with increase in the number of cycles in a parabolic way, resulting, after 10,000 cycles, in lower wear weight loss than the conventional hard chromium plating.
- Despite the fact that both hard chromium platings completed the salt spray tests with full corrosion after 72 hr, the increase in thickness enhanced the hard chromium protection from the salt spray corrosion.
- Salt spray test results for samples plated with 50 µm of accelerated hard chromium and electroless nickel underlayers 10, 20 and 30 µm thick indicate that no visual corrosion was observed for samples having electroless nickel underlayers 20 and 30 µm thick after 312 hr of testing.

References

1. B.E. Bodger, R.T.R. McGrann & D.A. Somerville, *Plat. & Surf. Finishing*, **84**, 28 (Sept. 1997).
2. J.M. Tyler, *Met. Finishing*, **93**, 11 (Oct. 1995).
3. D.C. Bolles, *Welding Journal*, **31** (1995).
4. K.O. Legg, *Plat. & Surf. Finishing*, **83**, 12 (July, 1996).
5. H.S. Kuo & J.K. Wu, *J. Mat. Sci.*, **31**, 6095 (1996).
6. J. Pina, A. Dias, M. Frangois & J. C. Lebrun, *Surf. & Coatings Technol.*, **96**, 148 (1997).
7. A.R. Jones, *Plat. & Surf. Finishing*, **76**, 62 (April, 1989).
8. S. Hotta, Y. Itou, K. Saruki & T. Arai, *Surf. & Coatings Technol.*, **73**, 5 (1995).
9. S. Wang, Y. Li, M. Yao & R. Wang, J. *Mater. Proc. Technol.*, **73**, 64 (1998).
10. Y. Matsumoto, D. Magda, D.W. Hoeppner & T.Y. Kim, *J. Eng. for Industry*, **113**, 154 (1991).
11. J-R. Hwang & C-P. Fung, *Surf. & Coatings Technol.*, **80**, 217 (1996).
12. J. Chitty, A. Pertuz, H. Hintermann, M.H. Staia & E.S. Puchi, *Thin Solid Films*, **308**, 430 (1997).
13. J.A. Berrios, M.H. Staia, E.C. Hernandez, H. Hintermann & E.S. Puchi, *Surf. & Coatings Technol.*, **108**, 466 (1998).
14. H. Wang, W. Xia & Y. Jin, *Wear*, **195**, 47 (1996).
15. O.A. Ashiru & J. Shirokoff, *Appl. Surf. Sci.*, **103**, 159 (1996).
16. Y. Wu, Y. Zhang & M. Yao, *Plat. & Surf. Fin.*, **82**, 83 (April, 1995).
17. R.N. Duncan, *Proc. VIII EBRATS*, 139 (1994).
18. A. Horsewell, *Mater. Sci. & Technol.*, **14**, 549 (1998).
19. E. Budke, J. Krempel-Hesse, H. Maidhof & H. Schüssler, *Surf. & Coatings Technol.*, **112**, 108 (1999).
20. Y. Sugimura & S. Sureih, *Fatigue of Coated Materials: Ceramic Coating*, **44**, 9 (1993).
21. U. Wiklund, P. Hedenquist & S. Hogmark, *Surf. & Coatings Technol.*, **97**, 773 (1997).

About the Authors

Marcelino Pereira do Nascimento is a doctoral candidate in mechanical engineering in the Materials and Technology Department of São Paulo State University–UNESP/FEG/DMT. He has specialized on the effects of surface treatment, such as shot peening, electroless nickel and hard chromium coatings on the mechanical properties (including fatigue and residual stresses) of high-strength steels, used in the aeronautical industry.

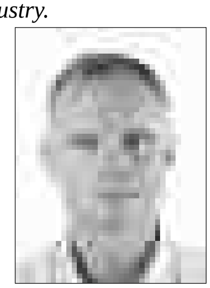

Dr. Herman Jacobus Cornelis Voorwald is a professor in the Materials and Technology Department of São Paulo State University–UNESP/FEG. He is a specialist in fracture, fatigue properties and strengthening of materials by surface treatments. He has published numerous papers on these subjects.

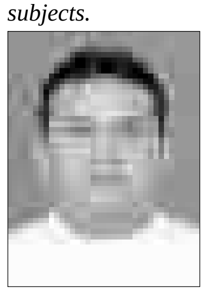

Renato Chaves Souza is a doctoral candidate in materials engineering in the Chemical Engineering Faculty Materials Department–FAENQUIL/DEMAR–Lorena/SP/BR. He has specialized in HVOF/HP thermal spray coating effects on fatigue behavior of high-strength steel used in the aeronautical industry.

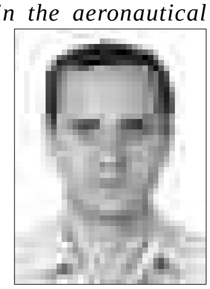

Walter Luis Pigatin is a senior engineer at EMBRAER-LIEBHERR/EDE Equipment Division (Brazilian aeronautical industry), São José dos Campos, Brazil. He is responsible for the heat treatment and surface coating of landing gear components in the material division.